The Journal of

IMAGING SCIENCE and TECHNOLOGY

Gamut Mapping to Preserve Spatial Luminance Variations

Raja Bala, Ricardo deQueiroz, Reiner Eschbach, and Wencheng Wu
Xerox Research & Technology, New York

IS&T
The Society for Imaging Science and Technology
7003 Kilworth Lane, Springfield, VA 22151
703-642-9090; FAX: 703-642-9094
E-mail: info@imaging.org

Gamut Mapping to Preserve Spatial Luminance Variations

Raja Bala,▲ Ricardo deQueiroz, Reiner Eschbach,▲ and Wencheng Wu▲

Xerox Research & Technology, Webster, New York

A spatial gamut mapping technique is proposed to overcome the shortcomings encountered with standard pointwise gamut mapping algorithms by preserving spatially local luminance variations in the original image. It does so by first processing the image through a standard pointwise gamut-mapping algorithm. The difference between the original image luminance Y and gamut mapped image luminance Y' is calculated. A spatial filter is then applied to this difference signal, whose output is added back to the gamut mapped signal Y'. The filtering operation can cause some pixel colors that lie near the gamut boundary to be moved outside of the gamut, hence a second gamut mapping step is required to move these pixel colors back into the gamut. Finally, all pixels are processed through a color correction function for the output device, and rendered for that device. The algorithm is designed to reduce many of the artifacts arising from standard pointwise techniques. Psychophysical experiments indicated an observer preference for the proposed algorithm.

Journal of Imaging Science and Technology 45: 436-443 (2001)

Introduction

Gamut mapping is an important problem in color management, and has been one of the most active areas of color research.[1–12] The optimal gamut mapping strategy for a given application depends on input and output gamuts, image content, user intent and preference. The design of the optimal technique thus involves a suitable trade-off among image attributes such as contrast, luminance detail, vividness, and smoothness. A plethora of gamut mapping algorithms has been proposed in the literature, optimized for different applications, and with different trade-offs. An overview of the work in this area along with an extensive list of references, can be found in the manuscripts by Morovic[1] and Braun.[2]

One might classify gamut-mapping algorithms into three basic categories. The first category comprises device dependent algorithms, wherein the gamut mapping is a function of the input (usually computer display) and output (usually printer) gamuts. These algorithms are independent of input image content. Most well-known gamut mapping algorithms fall in this category.[1,3–6]

The second category consists of image dependent algorithms, wherein the gamut mapping is a function of the input image statistics, and of the output device gamut. These algorithms are generally expected to perform better than image independent algorithms because they can adapt to image content[2,7,8] at added computational cost.

Original manuscript received January 26, 2001

▲ IS&T Member

Author contact info: Ph: 716 265 7838; Fax: 716 422 6117; Email: RBala@crt.xerox.com

Color Plate 2 is printed in the color plate section of this issue, p. 482.

In these first two categories, the gamut mapping is a pointwise operation from an input point to an output point in an appropriate (usually perceptual) 3D color space. One of the fundamental attributes of pointwise operations is that they do not take spatial neighborhood effects into account. In certain situations, these neighborhood effects can be of high importance. For example, consider an image composed on the computer display (CRT), with black text against a blue background. The text is easily distinguished against the background. However, when both are mapped to a printer's gamut with an algorithm that maps out-of-gamut colors to the nearest surface color, the CRT blue maps to a much darker blue in the printer's gamut. On the other hand, the CRT black maps to a lighter printer black. This is illustrated in Fig. 1, where the dotted and solid gamuts represent the CRT and printer respectively, and the nearest point mapping is labeled GM1. As a result of this gamut mapping, much of the luminance distinction is lost between text and background, and the legibility of the text is diminished. A comparison of luminance profiles of the input and resulting printed images is shown in Fig. 2. Note that such a gamut mapping function is considered optimal when rendering large areas of black or blue in isolation, so that the problem is only encountered when the two regions are juxtaposed. One can alleviate this problem by adopting a different pointwise gamut-mapping algorithm that preserves luminance (labeled GM2 in Fig. 1). Now the visibility of the text will greatly improve, but luminance preservation usually comes at the cost of significant loss in chroma, and this will likely be unacceptable in a different image or even different image area. Hence, all pointwise algorithms are heavily constrained by such trade-offs, making it difficult to develop a common algorithm that achieves high quality for a large variety of images and gamuts.

The third category of gamut mapping algorithms, which is the focus of this article, consists of algorithms that take into account the spatial characteristics in ad-

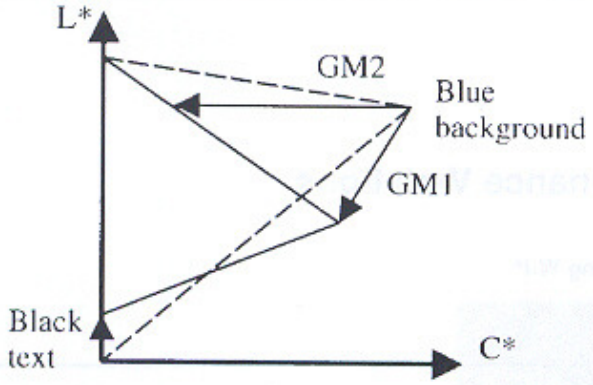

Figure 1. Mapping of black text and blue background from CRT gamut (dashed line) to print gamut (solid).

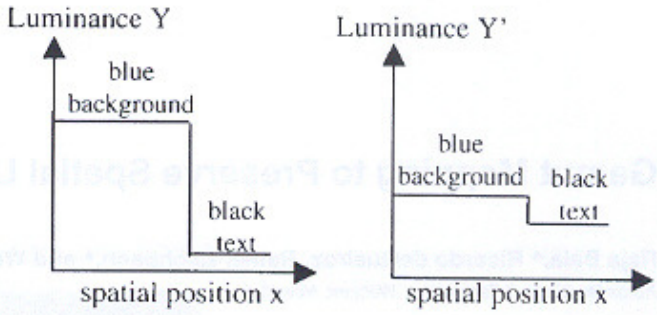

Figure 2. Spatial luminance profile of the gamut mapping shown in Fig. 1.

dition to color characteristics of the image. We believe not many algorithms exist in this class. With such algorithms, two pixels of the same color in an input image might map to different colors in the output image, depending on the spatial characteristics in their respective spatial neighborhood. A few researchers have proposed techniques in this category. Meyer and Barth[9] used homomorphic filtering to separate low and high spatial frequency channels, and then to apply global dynamic range compression only to the low frequency channel. A potential problem with such approaches that separate spatial from color transformations is that they are susceptible to noise amplification. Kasson[10] proposed a blending of two gamut mapping algorithms, one preserving luminance and one preserving chrominance. The blending is a function of distance from gamut, and spatial frequency, with luminance being preserved at high frequencies, and chrominance preserved at low frequencies. McCann[11] used the principles of Retinex theory to develop an iterative gamut mapping which attempts to preserve ratios of colors at adjacent pixels.

In this article, we propose a spatial gamut mapping technique, which is intended to mitigate the trade-off between luminance and chrominance preservation by incorporating the pixel neighborhood into the mapping. This article is a more complete description of a recent conference proceeding.[12]

This article is organized as follows. In the next section, the spatial gamut-mapping algorithm is described. In the following section, a psychophysical experiment is presented that evaluates the spatial algorithm in comparison to standard pointwise techniques. This is followed by an analysis of the results, and concluding remarks.

Gamut Mapping with Spatial Feedback

In this section, we describe a spatially dependent gamut mapping algorithm based on the principle that it is more important to preserve luminance at high spatial frequencies, while it is generally desirable to preserve chrominance at low spatial frequencies.[13] Our proposed method tightly couples the spatial and color transformations in a corrective feedback mechanism, resulting in a robust framework for gamut mapping.

In the following discussion, the term "luminance" is used generically encompassing the strict definitions of luminance, i.e., the Y component in XYZ, and lightness, i.e., the L^* component in CIELAB. The chrominance components C_1 and C_2 are likewise a generic representation of opponent color signals. Gamut mapping operations take place in such a device independent luminance–chrominance space.

A block diagram of the proposed algorithm is shown in Fig. 3. Let us define G_1 as a pointwise gamut clipping algorithm that emphasizes preservation of chroma over luminance. Let G_2 be another pointwise gamut clipping algorithm that emphasizes preservation of luminance over chroma. First G_1 is applied to the input colors, and an error image ΔY is computed between the luminances of the input signal Y and gamut mapped signal Y'. A spatial filter F is applied to the error image, resulting in image $\Delta Y'$. Here, F has high-pass frequency characteristics, i.e., it preserves the high spatial frequencies while suppressing the low spatial frequency components of the signal ΔY. The error image, which comprises only the high frequency errors introduced by gamut mapping, is then added back to the gamut mapped signal Y' to yield signal Y''. The feedback step may move some pixel colors (Y'' C_1' C_2') out of the gamut, and hence, a second gamut mapping operation G_2 is applied to limit all colors to the intended gamut. The proposed algorithm exhibits the following characteristics:

- If a region in the image is completely within the gamut, then G_1 is an identity function; $\Delta Y = \Delta Y' = 0$; and G_2 is an identity function. Hence this region of the image is unaltered.
- If a region in the image is outside the gamut, and is smoothly varying (*i.e.* of low frequency), G_1 will restrict colors to the gamut; ΔY will be a low frequency signal, therefore its high frequency component, $\Delta Y'$ will be close to zero; and G_2 will be essentially an identity function. Thus, the overall mapping in this region is predominantly G_1.
- If a region in the image is outside the gamut, and contains high frequency detail, then ΔY will contain some high frequency components; these components will be extracted by the filter as $\Delta Y'$; the feedback will move colors out of gamut; and the second gamut mapping G_2 will take effect. Hence in this case, the overall mapping is predominantly G_2.

In summary, the proposed scheme leads to the preservation of the characteristics of G_1 in low spatial frequencies and those of G_2 in high spatial frequencies. Hence the strengths of both algorithms are exploited in the appropriate spatial frequency bands, and the trade-offs that one must face with pointwise algorithms are now

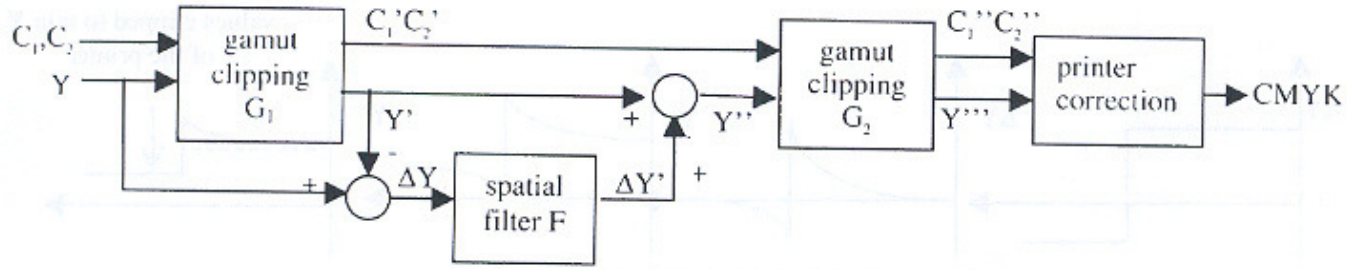

Figure 3. Block diagram of proposed spatial gamut mapping algorithm.

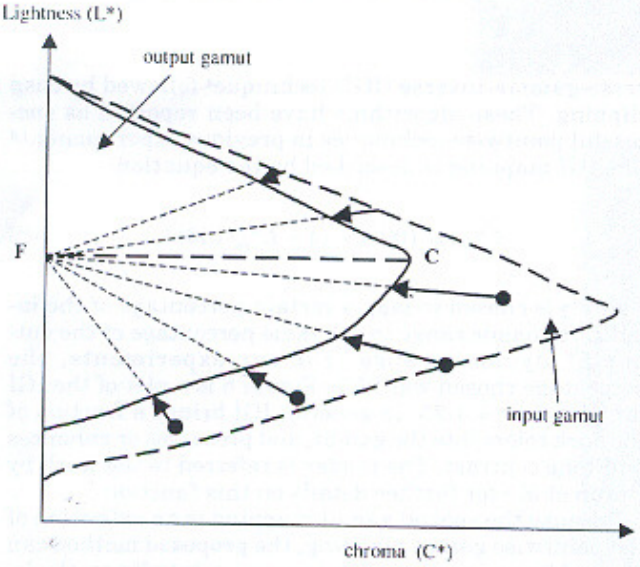

Figure 4. Cusp gamut clipping algorithm shown at a fixed hue angle (CIELAB $H = 40$). C is the cusp at the given hue plane. F is the neutral focal point for all gamut mapping vectors in the given hue plane. The input gamut is that of a Xerox DocuColor12 xerographic printer, and the output gamut is that of a Xerox Xpress inkjet printer.

significantly mitigated. All the operations up to this point constitute the overall spatial gamut-mapping algorithm, performed in a device independent luminance–chrominance space. The final step is to convert device independent color to device dependent color (i.e., CMYK) via a printer color correction transform.[14] To reduce the overall computational complexity of the algorithm, G_1 can be implemented using a 3-D lookup table, and G_2 can be concatenated with the printer color correction transform from CIE color to CMYK.

The design of G_1 and G_2, and the spatial filter F can depend on many factors, including global and local image characteristics, device characteristics, rendering intent and preference. We will describe an initial implementation in this article, recognizing that more research will be needed to further optimize the algorithm parameters. For this article, the gamut mapping G_1 was chosen to map out-of-gamut colors to the nearest surface point of the same hue. This mapping generally favors preservation of chroma over luminance. For G_2, the cusp algorithm was chosen where out-of-gamut colors are mapped to the surface in a direction towards a neutral point whose luminance is that of the cusp color.[1] (The cusp is defined as the point of maximum chroma in a given hue slice.) Figure 4 is an illustration of the cusp algorithm for the input and output gamuts actually used in the experiments. This algorithm tends to emphasize luminance over chroma preservation, especially for points close to the gamut surface. Another alternative for G_2 is a mapping that clips out-of-gamut colors to surface colors of the same luminance. In our initial experiments, we found that this yielded results very similar to cusp clipping when used in the framework of Fig. 3. Moreover, one may wish, for cost or performance considerations, to disable the spatial component of the gamut mapping (namely G_1 and F in Fig. 3), and apply only G_2 for gamut mapping. We found that in this case, cusp clipping does not desaturate the image as much as constant-luminance clipping, and is hence preferable. For these reasons, cusp clipping was finally chosen for G_2.

Both G_1 and G_2 leave in-gamut colors unaltered. While the chosen G_1 yields high-chroma reproductions, it is susceptible to the "lightning rod effect", where-in several image colors map to one point, especially near black and at the gamut cusp. In the proposed technique, if these image colors are from a high spatial frequency region, the filtered feedback will redistribute their luminance values, and G_2 will retain luminance distinction, thus eliminating the problem.

Figure 5 demonstrates what happens at various points in the algorithm for the example of blue text on black background (see Figs. 1 and 2). Adding the filtered error $\Delta Y'$ to the gamut mapped luminance Y'' yields the signal Y''', which retains the characteristics of the original input image Y near the edge while retaining the characteristics of the gamut mapped image Y'' in smooth regions (see Fig. 2). This signal, in combination with the chrominance signals C_1' and C_2' must be remapped to the gamut surface with the transform G_2, to yield a luminance profile Y'''' which may be somewhat different from Y'''. In this example, Y''' contains luminances that are below the minimum luminance achievable by the printer, hence these values get clipped. However, even with this limitation, the algorithm restores the edge information that was diminished in the pointwise algorithm (shown as a dashed line in the rightmost plot in Fig. 5). The extent and spatial footprint of the enhancement is dependent directly on the characteristics of the high-pass filter F. In this article, we have chosen a simple linear filter whose operation at pixel i is given by:

$$\Delta Y_i' = k\left(\Delta Y_i - \frac{1}{N^2}\sum_{j\in S}\Delta Y_j\right), \qquad (1)$$

where, k is the filter gain, N is the filter size, and S is an $N \times N$ neighborhood around pixel i. Eq. 1 says that the filter is subtracting a low frequency component (i.e., the $N \times N$ neighborhood average) from the signal, and thus retaining the remaining high frequency compo-

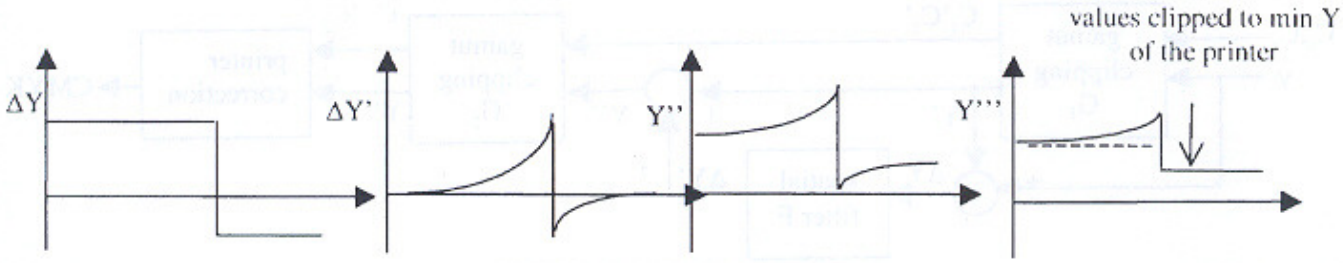

Figure 5. Spatial luminance profile of black text and blue background of Figs. 1 and 2 at the various stages in the proposed algorithm.

nents. With these characteristics, the overall gamut mapping, with spatially filtered feedback, will approximately reproduce the variations in Y at high spatial frequencies, while reducing to the pointwise mapping G_1 at low spatial frequencies.

As might be expected, the filter gain k and filter size N will dictate the outcome and efficacy of this spatial gamut mapping technique. With a high gain in filter F, the luminance Y at the regions of high spatial frequencies is preserved or even enhanced. However, this comes at the cost of strongly distorting the chrominances at those regions. If a low filter gain is used, the effect of luminance preserving at the regions of high spatial frequencies might be unnoticeable. The filter size N determines the cut-off frequency between high and low spatial frequencies as well as the spatial extent of the filtering effect. The optimal N generally depends on the image type. For images with soft or noisy edges, e.g. scanned pictorials, a relatively large filter size, such as $N = 15$ (at 600 dpi), is required for noticeable improvement. On the other hand, for images that have strong edges and low noise, e.g. computer generated business graphics, a large filter size produces distinct halo effects around edges; hence a smaller filter size, such as $N = 3$ (at 600 dpi), is preferable. In general, if the image type is known *a priori*, the algorithm should use this information to switch between the small and large filter sizes. If this is not the case, an adaptive scheme can be applied to accomplish the selection of the filter size. Preliminary work on adaptive filtering was described in a previous article.[12] The main focus of this manuscript, however, is spatial gamut mapping of scanned pictorial imagery. From our experiments on a Xerox DocuColor12 xerographic CMYK printer with 600 dpi resolution, a filter gain $k = 1$ and a filter size $N = 15$ was empirically chosen. Automatic optimization of k and N as a function of image type, image resolution, etc. is an area of ongoing research.

Psychophysical Evaluation of Spatial Gamut Mapping

The ultimate goal of gamut mapping is to create an output image that is a visually preferred rendition of the original. It is important, thus, to ensure that human observers evaluate the performance of the gamut mapping technique. To this end, a visual experiment was conducted to compare the spatial gamut mapping technique with a selected set of previously published algorithms on a set of pictorial images.

Description of the Algorithms

The spatial gamut mapping was compared with two standard pointwise techniques, which were: (i) clipping to the nearest point on the gamut surface while preserving hue; and (ii) nonlinear L^* compression using the inverse-gamma-inverse (IGI) technique[4] followed by cusp clipping. These algorithms have been reported as successful pointwise techniques in previous experiments.[1,4] The IGI mapping is described by the equation:

$$L^*_{out} = 100(1 - (1 - L^*_{in}/100)^{\gamma}), \qquad (2)$$

where γ is chosen to map a certain percentage of the input L^* dynamic range to the same percentage of the output L^* dynamic range. For our experiments, the percentage chosen was 95%. Figure 6 is a plot of the IGI function for $\gamma = 1.25$. In general, IGI brings a fraction of the dark colors into the gamut, and preserves or enhances mid-tone contrast. The reader is referred to the work by Braun et al.[4] for further details on this function.

Because the spatial gamut mapping is an extension of the pointwise gamut mapping, the proposed method can be used in conjunction with common pointwise methods. Thus, two versions of the spatial gamut mapping method were tested. The first version was exactly as depicted in Fig. 3, with the operations G_1, G_2, and F implemented as described in the previous section. Because the images were all pictorials, the filter size was chosen to be $N = 15$. CIELAB was used as the luminance–chrominance space. Because G_1 is identical to nearest-point mapping (NP), this first version is in effect a spatial extension of NP. In the second version, IGI L^* compression was applied in addition to the spatial operation. There are several possible locations in Fig. 3 where L^* compression can be applied. These are shown in Fig. 7 as dashed gray blocks. The compression can be applied as a preprocessor before the proposed algorithm (i.e., L_1). Alternatively it can be applied just prior to G_1 (i.e., L_2), in which case its effect is included in the error image calculation. Finally, it can be applied just prior to G_2 (i.e., L_3). The second alternative can lead to potentially undesirable interactions between L^* compression of in-gamut pixel colors and the spatial filter F. Intuitively, the third alternative is unappealing since the spatial feedback is applied with no knowledge of a subsequent global color adjustment (i.e., IGI). Hence, the first alternative was chosen, i.e., IGI was applied at location L_1 as a global preprocessing step, followed by spatial gamut mapping, which is a correction that is local in both spatial and color coordinates.

For convenience, we adopt the following symbols for the four algorithms: NP, IGI_CUSP, SGM, IGI_SGM. Table I lists the components of the four algorithms with respect to the block diagram of Fig. 3.

Stimuli

Five pictorial scenes were used, whose grayscale versions are shown in Fig. 8. These scenes represent a broad

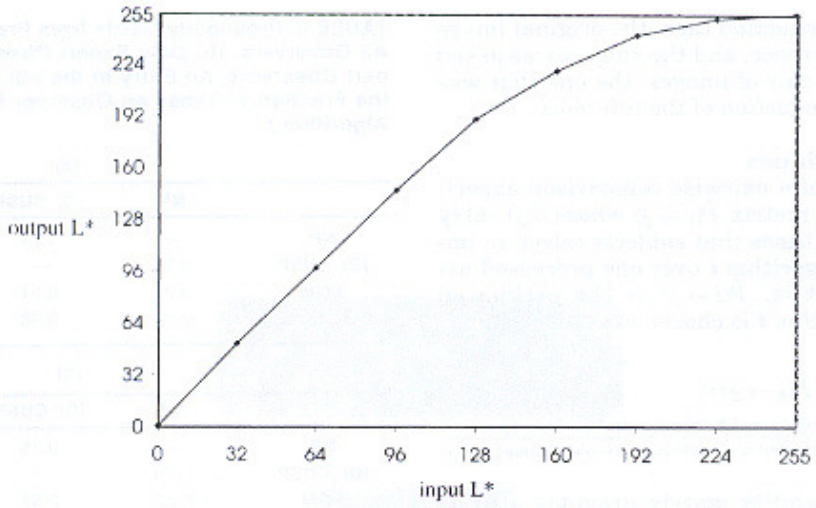

Figure 6. Plot of the inverse-gamma-inverse (IGI) function for $\gamma = 1.25$. (The L^* values are scaled to occupy the range 0–255.)

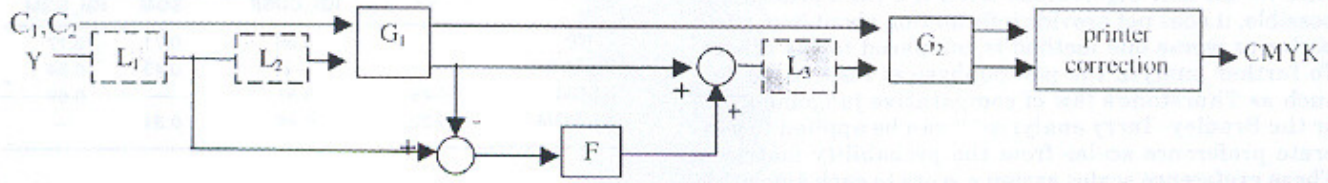

Figure 7. Block diagram of spatial gamut mapping algorithm showing the various alternatives for L^* compression, L_1, L_2, L_3.

Figure 8. Grayscale versions of images used in psychophysical experiment.

TABLE I. Components of the Different Gamut Mapping Methods Used in the Psychophysical Experiments

	L^* compression	G_1	Filter Feedback	G_2
NP	None	Nearest Point	None	None
IGI_CUSP	IGI	None	None	Cusp
SGM	None	Nearest Point	High-Pass	Cusp
IGI_SGM	IGI	Nearest Point	High-Pass	Cusp

range of pictorial imagery, and include smooth and textured regions, flesh tones, pastels, neutrals, highlights, shadows, and saturated colors of many different hues. For each scene, the original and the four gamut-mapped versions were printed on a Xerox DocuColor12 printer. The prints were of size 5" × 7". The printer was calibrated for matching under D50 illuminant, and the images were displayed in a light booth under D50 illuminant. The illumination level within the booth was 2300 lux. The viewing distance was approximately 20". All ambient illumination in the room was turned off. The gamut-mapped versions were restricted to a smaller gamut of a Xerox Xpress inkjet printer. By using the same printer for original and gamut-mapped versions, cross-printer and cross-media problems such as metamerism could be avoided.

Experimental Procedure

A total of 18 observers participated in the visual experiments. Among these, 11 were experts and 7 were non-experts in terms of experience in color imaging. All observers reported normal color vision.

Two psychophysical experiments were conducted. One used visual preference and the other used accuracy of reproduction, as the quality criterion. The technique of pair-wise comparison was used in both experiments. In the preference task, the subject was presented with a pair of images corresponding to two gamut-mapping algorithms, and asked to select the most preferred image. This was repeated for every possible pair of images, for each of the

five scenes. In the reproduction task, the original image was presented as a reference, and the subject was asked to select, from a given pair of images, the one that was the more accurate reproduction of the reference.

Data Analysis Techniques

The direct outcome of a pairwise comparison experiment is the probability matrix $\hat{P}(i \to j)$ whose (i,j) entry denotes the fraction of times that subjects select an image processed using algorithm i over one processed using algorithm j. That is, $\hat{P}(i \to j)$ is the estimated probability that algorithm i is chosen over algorithm j:

$$\hat{P}(i \to j) = \frac{\text{The number of occurrences that algorithm } i \text{ is preferred over } j}{\text{The total number of comparisons that are made between algorithms } i \text{ and } j}$$

The estimated probability matrix provides a first-order observation about the performance of each method compared with every other method, a pair at a time. However, it does not directly provide an ordering of preference for all four algorithms. Even if a rank ordering is possible, it does not provide information about how much better or worse one method is compared to the others. To further analyze the psychophysical results, models such as Thurstone's law of comparative judgement,[15,16] or the Bradley–Terry analysis[17,18] can be applied to generate preference scales from the probability matrices. These preference scales assign a score to each algorithm that indicates its performance relative to the other algorithms. The differences between the aforementioned two models are in the form of their underlying probability distribution functions (Thurstone uses a cumulative Gaussian function, while Bradley–Terry uses a logistic function), and the method of estimating the preference scales (Thurstone uses least-squares estimates, while Bradley–Terry uses maximum-likelihood estimates). In the authors' experience, the outputs of these models are quite similar; however, the Bradley–Terry formulation has been more fully developed from a statistical viewpoint, and offers hypothesis testing and estimates for confidence intervals. Hence, we adopted that model to analyze our experimental data. For a detailed description of the Bradley–Terry model, and comparisons with the Thurstone model, see Ref 18.

Results and Discussions

For illustration purposes, **Color Plate 2 (p. 482)** shows the original and four gamut-mapped reproductions for one of the scenes, "macaws", used in the experiment. In order to fit all the images onto one figure for easy comparison, a small interesting region has been cropped from this scene. It must be noted that additional processing to prepare prints for this journal may result in some loss in color accuracy; however, it is hoped that the salient points about the algorithms will be retained. First, a comparison of images (A) and (B) shows that shadow detail around the beak, and high-chroma detail in the red feathers have been eliminated by nearest point clipping (NP). IGI L^* compression in image (C) has overall lightened the image. This is effective in bringing out the shadow detail. It also restored high-chroma detail, but did so at the expense of an overall loss in chroma. Spatial gamut mapping in image (D) is a spatial extension of (B); it is easily seen that much of the high-chroma detail was restored without a substantial sacrifice in chroma. A combination of IGI compression and spatial gamut mapping in image (E) shows the benefit of both components, i.e., restoration of shadow detail around the beak, as well as restoration of high-chroma detail in the feathers.

TABLE II. Probability Matrix from Preference Experiment: (a) All Observers; (b) Only Expert Observers; (c) Only Non-Expert Observers. An Entry in the *i*-th Column and *j*-th Row is the Fraction of Times an Observer Picked Algorithm *i* Over Algorithm *j*.

(a)

	NP	IGI_CUSP	SGM	IGI_SGM
NP	—	0.71	0.63	0.76
IGI_CUSP	0.29	—	0.49	0.62
SGM	0.31	0.51	—	0.71
IGI_SGM	0.24	0.38	0.29	—

(b)

	NP	IGI_CUSP	SGM	IGI_SGM
NP	—	0.75	0.67	0.75
IGI_CUSP	0.25	—	0.49	0.67
SGM	0.33	0.51	—	0.73
IGI_SGM	0.25	0.33	0.27	—

(c)

	NP	IGI_CUSP	SGM	IGI_SGM
NP	—	0.66	0.71	0.77
IGI_CUSP	0.34	—	0.49	0.54
SGM	0.29	0.51	—	0.69
IGI_SGM	0.23	0.46	0.31	—

Results from the Preference Experiment

The probability matrices for the preference experiment are listed in Table II. From Table II(a)–(c), it can be seen that the columns labeled as "IGI_SGM" have all entries that are substantially greater than 0.5 for both the expert and non-expert groups. Because a tie in a pair-wise comparison has probability 0.5, IGI_SGM is a clear winner under the preference criterion when compared to the other three methods independently. The results in Table II also indicate that NP is the worst method among all the four techniques.

The Bradley–Terry scales, calculated from data in Table II, and their 95% confidence intervals are shown in Fig. 9(a) (see Ref. 18 for details). From this figure, we see that IGI_SGM is the most preferred method, while NP is the least preferred. This is in agreement with the probability matrix in Table II. In comparing NP with SGM, and IGI_CUSP with IGI_SGM respectively, we see that introduction of the spatial mapping step consistently results in an improvement. Also, respective comparisons of NP with IGI_CUSP and SGM with IGI_SGM suggest that IGI compression tends to improve preference scores. This is probably because the L^* compression tends to lighten the images, an effect that is generally desirable in gamut mapping.[19] A combination of IGI and spatial mapping tends to inherit the advantages of both approaches, thus yielding the highest preference score. Finally, both expert and non-expert groups yield very similar trends.

Results from the Reproduction Experiment

The probability matrix for the reproduction experiment is given in Table III. From Table III(b) it can be seen that the column labeled as "SGM" has all entries substantially greater than 0.5. That is, for the experts,

TABLE III. Probability Matrix from Reproduction Experiment: (a) All Observers; (b) Only Expert Observers; (C) Only Non-Expert Observers. An Entry in the *i*-th Column and *j*-th Row is the Fraction of Times an Observer Picked Algorithm *i* Over Algorithm *j*.

(a)

	NP	IGI_CUSP	SGM	IGI_SGM
NP	—	0.49	0.68	0.47
IGI_CUSP	0.51	—	0.62	0.52
SGM	0.32	0.38	—	0.44
IGI_SGM	0.53	0.48	0.56	—

(b)

	NP	IGI_CUSP	SGM	IGI_SGM
NP	—	0.44	0.71	0.44
IGI_CUSP	0.56	—	0.65	0.47
SGM	0.29	0.35	—	0.36
IGI_SGM	0.56	0.53	0.64	—

(c)

	NP	IGI_CUSP	SGM	IGI_SGM
NP	—	0.57	0.63	0.51
IGI_CUSP	0.43	—	0.57	0.60
SGM	0.37	0.43	—	0.57
IGI_SGM	0.49	0.40	0.43	—

SGM is a clear winner under the reproduction criterion. No method is clearly the worst technique. For non-experts, the results presented in Table III(c) are inconclusive. According to Table III(c), "IGI_SGM" is the best; and the "NP" is the worst. However, the "IGI_SGM" is only slightly better than "NP" with the probability of 0.51. This difference could be simply due to noise, which is inevitably present in psychophysical data.

Looking at the Bradley–Terry scores in Fig. 9, we see that SGM outperforms the other algorithms. This trend is even stronger among the expert observers. The differences among the remaining three algorithms are not statistically significant. It appears that the expert group paid careful attention to fine image detail, which was successfully restored by SGM. For the non-experts, all four reproductions were essentially the same. With the feedback we received from some of the observers, we conclude that this trend is probably caused by the fact that all the reproductions were visually so different from the original reference image that casual observers could not distinguish among them. Generally speaking, the spatial algorithms performed better than their pointwise counterparts because they effectively retained detail and edge information in shadows and high-chroma regions that is often lost with standard techniques. L^* compression resulted in improved performance in the preference experiments, presumably due to an increase in perceived overall lightness, colorfulness, and contrast of the images. However, this was not the case in the reproduction experiment, presumably because the color changes just mentioned would result in a less accurate match to the original image.

Conclusions

We have presented a gamut-mapping algorithm that takes into account spatial characteristics of the image. This feature eliminates some of the compromises necessitated by standard pointwise algorithms. By closely coupling the spatial and color transformations in a corrective feedback mechanism, our approach does not suffer from the noise amplification problems that can arise when the two transformations are applied separately. Psychophysical experiments indicate that the proposed algorithm outperforms standard pointwise gamut mapping methods for pictorial images. Because the spatial algorithm is an extension of pointwise mappings, it will need to be continually evolved as improved pointwise methods are developed.

We believe that with some extensions, the algorithm will be equally effective for business graphics images. For example, while we have used high frequency luminance preservation as the criterion for spatial feedback, other criteria such as saturation or purity may be better suited for graphics imagery. Another important extension of this work is the adaptive optimization of the spatial filter for different image characteristics. Finally, while our method is likely to achieve results that are qualitatively similar to that obtained by Kasson and McCann, we believe our algorithm requires a simpler implementation and fewer computations than either of these approaches.

Acknowledgment. The authors would like to thank John Handley at Xerox Corporation for his valuable input on psychophysical analysis techniques. Many thanks go to Dean Harrington, also at Xerox Corporation, for conducting the psychophysical experiments. Finally the authors would like to thank the referees for their helpful comments and suggestions towards improving the quality of this article.

References

1. J. Morovic, *To develop a universal gamut mapping algorithm*, Ph. D. Thesis, University of Derby, 1998.
2. G. Braun, *A paradigm for color gamut mapping of pictorial images*, Ph. D. Thesis, Rochester Institute of Technology, 1999.
3. N. Katoh, M. Ito and S. Ohno, Three-dimensional gamut mapping using various color difference formulae and color spaces, *J. Electronic Imaging*, **8**, 365–379 (1999).
4. K. Braun, R. Balasubramanian, and R. Eschbach, Development and evaluation of six gamut mapping algorithms for pictorial images, *Proc. IS&T/SID's 7th Color imaging Conference*, IS&T, Springfield, VA, 1999, pp. 144–148.
5. K. Braun, R. Balasubramanian and S. J. Harrington, Gamut mapping techniques for business graphics, *Proc. IS&T/SID's 7th Color imaging Conference*, IS&T, Springfield, VA, 1999, pp. 149–154.
6. L. MacDonald, J. Morovic and K. Xiao, A topographic gamut mapping algorithm based on experimental observer data, *Proc. IS&T/SID's 8th Color Imaging Conference*, IS&T, Springfield, VA, 2000, pp. 311–317.
7. C. Hung–Shing, M. Omamiuda and H. Kotera, Adaptive gamut mapping method based on image-to-device, *Proc. IS&Ts NIP 15, 1999 International Conference on Digital Printing Technologies*, IS&T, Springfield, VA, 1999, pp. 346–349.
8. G. J. Braun and M. D. Fairchild, General-purpose gamut mapping algorithms: Evaluation of contrast-preserving rescaling functions for color gamut mapping, *Proc. IS&T/SID's 7th Color Imaging Conference*, IS&T, Springfield, VA, 1999, pp. 167–172.
9. J. Meyer and B. Barth, Color gamut mapping for hard copy, *SID Digest* **89**, 86–89 (1989).
10. J. M. Kasson, Color image gamut-mapping system with chroma enhancement at human-insensitive spatial frequencies, US Patent 5,450,216 (1995).
11. J. McCann, Lessons learned from Mondrians applied to real images and color gamuts, *Proc. IS&T/SID's 7th Color Imaging Conference*, IS&T, Springfield, VA, 1999, pp. 1–8.
12. R. Balasubramanian, R. de Queiroz, R. Eschbach, and W. Wu, Gamut mapping to preserve spatial luminance variations, *Proc. IS&T/SID's 8th Color Imaging Conference*, IS&T, Springfield, VA, 2000, pp. 122–128.
13. K. T. Mullen, The contrast sensitivity of human colour vision to red–green and blue–yellow chromatic gratings, *J. Physiol.* **359**, 381–400 (1985).

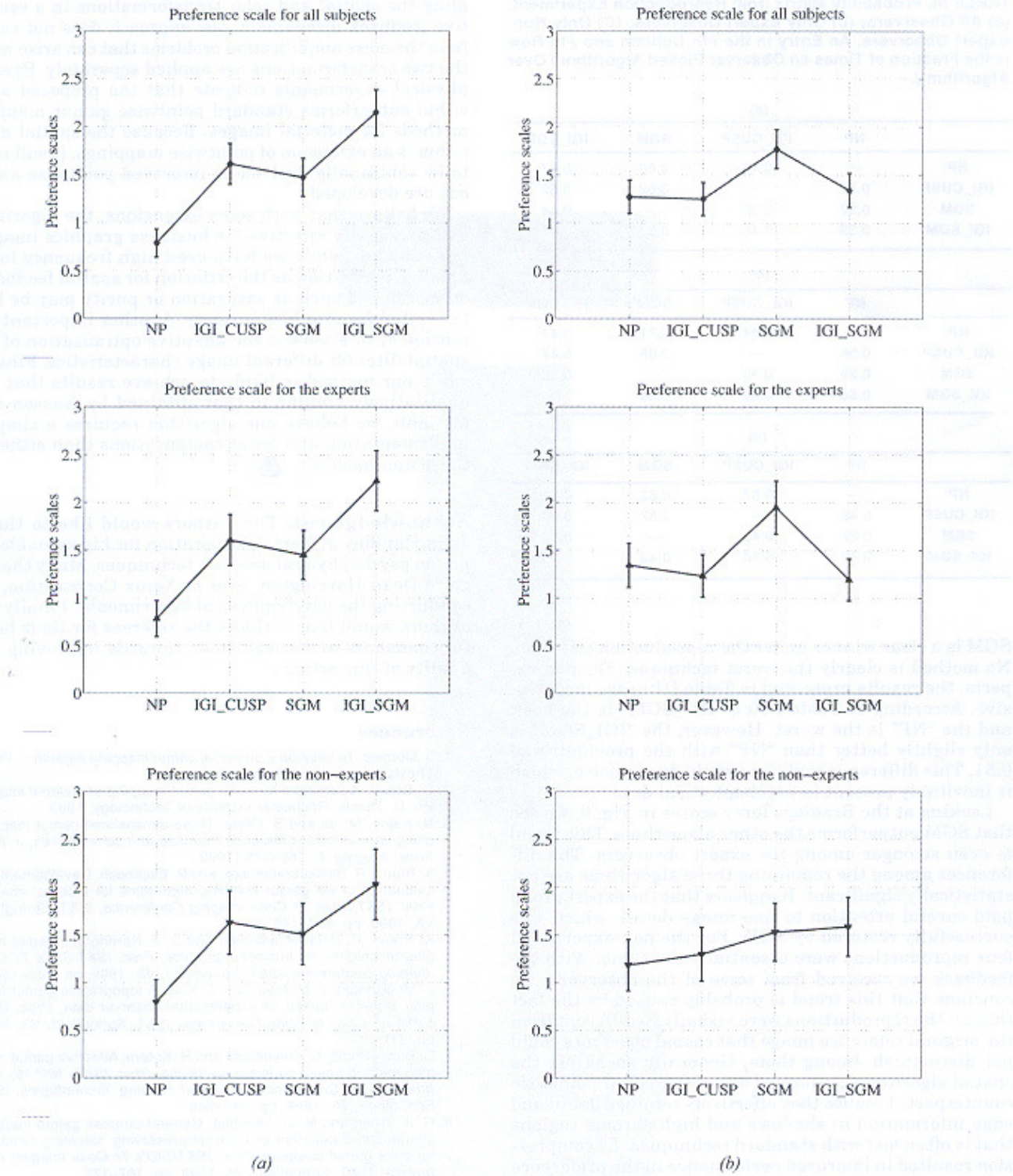

Figure 9. Preference scales from visual experiment for (a) preference and (b) reproduction experiment.

14. H. R. Kang, *Color Technology for Electronic Imaging Devices*, SPIE, Bellingham, WA, 1997, Chap. 12.
15. L. L. Thurstone, A law of comparative judgment, *Psych Rev.* **34**, 273–286 (1927).
16. K. M. Braun, M.D. Fairchild and P. J. Alessi, Viewing environments for cross-media image comparison, *Color Res. Appl.* **21**, 6–17 (1996).
17. R. A. Bradley, Paired comparison: some basic procedures and examples, *Handbook of Statistics*, **4**, 299–326 (1984).
18. J. C. Handley, Comparative analysis of Bradley–Terry and Thurstone–Mosteller paired comparison models for image quality assessment, *Proc. IS&T's Image Processing, Image Quality, Image Capture, Systems Conference*, IS&T, Springfield, VA, 2001, pp. 108–112.
19. B. Kang, M. Cho, J. Morovic, and M. R. Luo, Gamut compression algorithm development on the basis of observer experimental data, *Proc. IS&T/SID's 8th Color Imaging Conference*, IS&T, Springfield, VA, 2000, pp. 268–272.

(A)

(B) (C)

(D) (E)

Plate 2. Image "macaws" processed through various gamut mapping algorithms: (A) reference original, (B) NP, (C) IGI_CUSP, (D) SGM, (E) IGI_SGM. (Image source: Kodak PhotoCD sampler; photographer: Steve Kelly.) (Bala *et al.* pp. 436–443)